Ignition and Maintenance of Laser-Supported Detonation Waves

G. Weyl,* C. Rollins,* and D. Resendes†
Physical Sciences, Inc., Andover, Massachusetts 01810

Laser-driven detonation waves are being considered for use in ground to low-Earth-orbit launch applications. This paper addresses the problem of determining minimum laser irradiance for ignition and maintenance of laser-supported detonation waves. A means of igniting a detonation wave at low irradiance is to embed in the propellant thin metallic flakes that break down upon vaporization. A computational scheme has been developed for determining the structure and thickness of the waves. Results are presented for seeded H_2O, LiH, and glass propellants in the density range 10^{-4} to 10^{-2} g/cm^3.

Nomenclature

a	= flake radius
A	= area
C	= specific heat
c	= molar concentration, speed of light
D	= LSD wave velocity
d	= flake thickness
G_F	= gaunt factor
g, g^+	= degeneracy factor
H	= enthalpy per unit mass
H_v	= heat of vaporization
h	= Planck constant
I	= irradiance
I_0	= laser irradiance
k	= absorption coefficient
k_B	= Boltzmann constant
l	= thickness of LSD wave
M	= mass per unit area vaporized
$[M], [M^+]$	= concentration of specie M, M^+
N	= number density of flakes
N_{AV}	= Avogadro's number, 6×10^{23}
n	= number density
n_t	= defined by Eq. (7)
p	= pressure
R	= reflectivity
T	= temperature
U	= velocity
v	= thermal velocity
v_r	= radial velocity
X	= axial distance
y	= degree of ionization
z	= ion charge
α	= absorptivity
β	= mass fraction of flakes in propellant
γ, γ'	= coefficient of the adiabat defined by Eq. (10)
δ	= defined by Eq. (24)
ϵ_I	= ionization energy
ϵ_1	= energy of first excited state
η	= compression ratio ρ_0/ρ
λ	= wavelength
μ	= average molecular mass
ν	= frequency
ρ	= density
ρ_{0c}	= density, defined by Eq. (29)
σ	= cross section
τ	= time
ϕ_1	= fluence of first pulse
ϕ_H	= fluence to vaporize
χ	= inverse bremsstrahlung cross section
ω	= laser angular frequency

Subscripts

abs	= absorbed
br	= breakdown
CJ	= Chapman-Jouguet conditions
e	= electron
ei	= electron-ion
en	= electron-neutral
exp	= expansion
f	= flake
i	= ion
j	= specie j
L	= laser
m	= momentum transfer
ML	= Maxwell line
p	= propellant
S	= surface
sh	= shock
th	= threshold
V	= vapor
vbr	= vapor breakdown
0	= upstream conditions
1	= excited state

Superscripts

*	= edge of Knudsen layer

Received July 31, 1989; revision received March 1, 1990.

*Principal Research Scientist.
†Principal Scientist. Member AIAA.

Introduction

THE single-pulse laser-supported detonation wave rocket engine was introduced by Pirri and Weiss[1] in 1972. Douglas-Hamilton et al.[2] proposed the double-pulse version in 1978. In this concept a ground-based laser sends a beam that is focused onto the rear of a rocket engine, vaporizing and breaking down the propellant. The high temperatures and pressures thus generated can provide specific impulses in excess of 800 s. The laser generates a train of double pulses: The first pulse determines the amount of propellant that will be heated by evaporating a controlled amount of solid or liquid, and the second pulse ignites a detonation wave plasma[3] in the propellant. Thus, two laser pulses yield one thrusting pulse, and the resulting plasma expands away from the surface, becoming transparent before the next set of laser pulses.

The vapor/propellant flowfield associated with the double-pulsed laser supported detonation wave engine can be best described by separating it into four stages, three of which are shown schematically in Fig. 1. Stage 1 involves the blow off

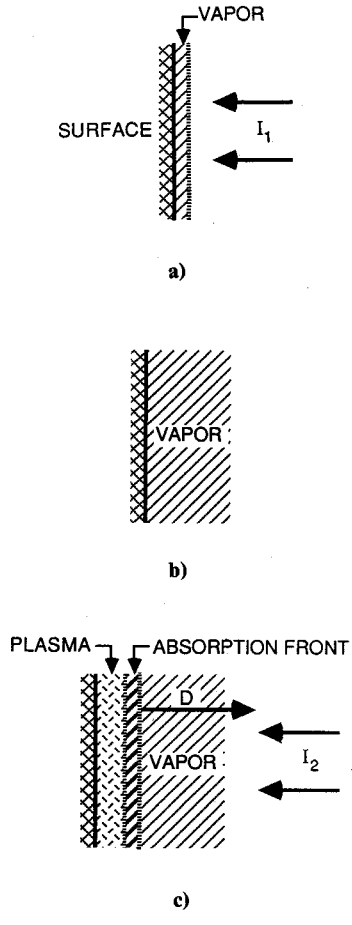

Fig. 1 First three stages in pulsed laser propulsion scheme: a) blow off of propellant vapor by first pulse; b) expansion of vapor after first pulse; c) ignition/propagation of LSD wave during second pulse.

by vaporization, sublimation, or pyrolysis/decomposition of a certain amount of propellant material when the first laser pulse is incident on the rear surface of the rocket. The second stage involves the expansion of the vapor during the time separation between the first and second pulses. The third stage involves the interaction of the second laser pulse with the vapor slab, and the last stage involves the expansion of the heated vapor/plasma into vacuum/air. The most interesting physics occurs during phase 3, when a plasma is ignited and evolves into a quasi-steady-state laser-supported detonation (LSD) wave[3] traveling at a velocity D with respect to the vapor in front of it. It is in this wave that the low-temperature vapor produced by the first pulse is processed by the second pulse into a high-temperature, high-pressure partially ionized gas (plasma).

Important issues that must be addressed for successful design and operation of a laser-propelled rocket are 1) the means of igniting the plasma and 2) the means in which the absorption front propagates through the vaporized fuel.

It is well known that aerosols can ignite plasmas at thresholds well below those for clean air breakdown. These plasmas may develop as LSD waves,[3] which grow laterally until they coalesce and block the laser beam.[4] One must find conditions under which ignition on the target will occur *without* any aerosol-induced breakdown. Figure 2 is a compilation of data taken at many places on aerosol-induced breakdown at 10.6 μ.[4] It shows the delay time to break down as a function of laser irradiance for a range of particle sizes. It is fortunate that the larger aerosol particles are only found near the ground. However, dust carried by and ejected from the rocket may pose a problem.

The object of the present studies is to devise means for lowering both the plasma ignition thresholds of the propellant and maintenance threshold of the LSD wave so that aerosol-induced breakdown and laser beam disruptions due to nonlinear effects in the atmosphere become insignificant. Calculations are performed at the wavelength of the CO_2 laser ($\lambda = 10.6\ \mu$), but results can readily be extended to shorter wavelengths by using the wavelength scaling of inverse bremsstrahlung absorption.[5]

Prompt Ignition of Plasma

This section presents a scheme for obtaining prompt ignition of plasmas at the beginning of the second pulse. It is based on the experimental finding[6] that aluminum surfaces, when submitted to CO_2 laser pulses ($\lambda = 10.6\ \mu$), would ignite plasma in air at very short times ($t \leq 50$ ns) when the laser irradiance exceeded 5×10^7 W/cm^2. The time was too short for the metal surface to start vaporizing, due to the large thermal conductivity of Al, and it was postulated that thermally insulated flakes, present on the surface, would vaporize over the times of interest and be plasma ignition sites. Electronmicrographs of Al surfaces were taken that indicated the presence of defects that could be construed as being flakes.[6] The theory of ignition off flakes was developed by Weyl et al.,[7] who confirmed that such defects could ignite plasmas over the times and irradiances that were used in the experiments.

The method proposed here to obtain rapid plasma ignition is to embed in the solid propellant a multitude of fine alu-

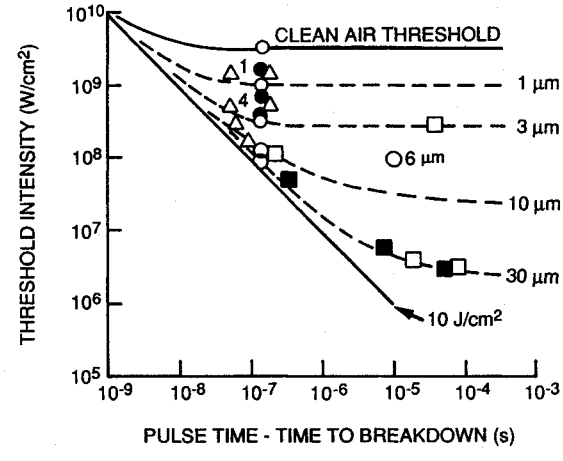

Fig. 2 Ignition thresholds in aerosol-laden air: $\lambda = 10.6\ \mu$.

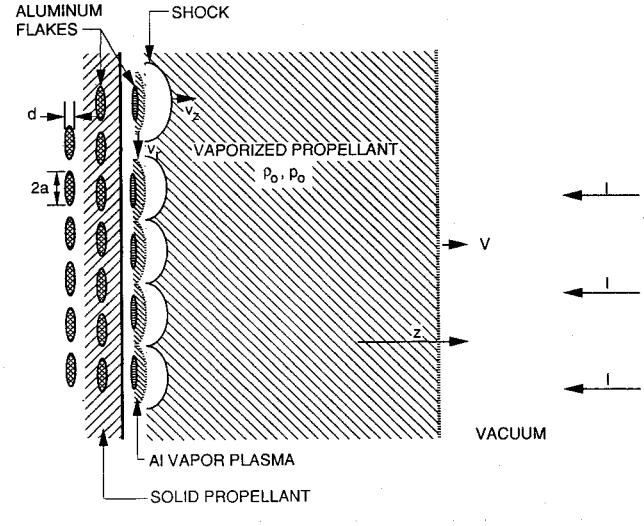

Fig. 3 Rapid plasma ignition over aluminum flakes embedded in the propellant.

minum flakes (thickness d, radius a). Rapid vaporization of the flakes and ignition of the aluminum vapor will occur at a threshold irradiance Ith of the order of 10^8 W/cm^2. The plasma ignition sites rapidly spread and overlap, serving as ignition sites for LSD waves that travel up the beam. The geometry is shown in Fig. 3.

Two conditions must be met for the ignition scheme to be practical: 1) The flakes must have retained their identity by the end of the first laser pulse (which ejects the propellant in order to form a vapor layer above the surface); and 2) the fluence required to ignite plasmas and to have them overlap must be small compared to the fluence required to drive the LSD waves through the vaporized fuel. Condition 2 will require a minimum threshold irradiance Ith and a minimum mass loading of aluminum flakes. It is also important that ignition occur at or near the surface. Once ejected, flakes will tend to travel with the vapor. However, we expect that, due to the high reflectivity of the flakes, ejection of the flakes will occur at a much later time than the start time of vaporization of unshielded propellant.

The physics for the analysis that follows is derived from a publication by Weyl et al.[7]

Heating of Flakes to Vaporization

The d is taken to be small enough that the flake is heated uniformly. The fluence per unit area required to heat the flake to its vaporization temperature is

$$\phi_H = \rho_f C d \Delta T \alpha^{-1} (= 3.2 \text{ J/cm}^2) \tag{1}$$

where in the last step we set $\rho_f = 2.7$ g/cm^3, $C = 1$ J/g-K, $d = 0.2\ \mu$, $\alpha = 0.05$, and $\Delta T = 3000$ K. Since the heat of vaporization of aluminum is 10 kJ/g, the fluence required for complete vaporization of the flake is three times larger (~ 10 J/cm^2) than ϕ_H given in Eq. (1).

Breakdown of the Aluminum Vapor

It was shown in Ref. 7 that, if one can break down the vapor before the expansion goes three dimensional, then the breakdown times are extremely short. The characteristic time (τ_{exp}) for three-dimensional vapor expansion is a/v. For $a = 5\ \mu$ and $T = 3500$ K ($v = 1.3 \times 10^5$ cm/s), we have $\tau_{\text{exp}} = 4 \times 10^{-9}$ s. If the laser irradiance is too low to cause breakdown over this time, then the expansion goes three dimensional, and a stationary shock forms around the flake that has the purpose of shocking back the overexpanded vapor so that the aluminum vapor stagnation pressure and the pressure of the background vaporized propellant are equal. The geometry for one- and three-dimensional expansions is shown in Fig. 2. Breakdown in the three-dimensional regime will occur in the shocked vapor (region 5 of Fig. 4b). Since the vapor density in region 5 of Fig. 2b is much lower than that in the one-dimensional expansion zone, the breakdown times will be much longer than those in the one-dimensional regime. It was shown in Ref. 7 that breakdown proceeds in two steps. In step 1 the electrons absorb laser radiation by inverse bremsstrahlung (IB) absorption and dump their energy into the first excited state (cross section σ_1) of aluminum at 3.14 eV above the ground state. During this stage the electron concentration remains constant and the population of the first excited state increases linearly with time. Phase 2 starts when the population of excited state is so high that electron impact ionization of the 3.14 eV state (cross section σ_I) becomes likely. This leads to rapid breakdown by electron avalanche. The delay to breakdown is well approximated by the duration of phase 1, which is

$$\tau_1 = \frac{(\sigma_1/\sigma_I)^{1/2}}{(2n_e n)^{1/2}} \frac{\epsilon_I}{\chi I} \tag{2}$$

where χ is given by[8]

$$\chi = \frac{4\pi e^2 \nu}{n m_e c(\omega^2 + \nu_m^2)} \simeq \frac{4\pi e^2 \nu_m}{n m_e c \omega^2} \tag{3}$$

The collision frequency (for momentum transferring ν_m) can be estimated from the work of Hyman et al.[9]:

$$\frac{\nu_m}{n} = 10^{-7} \quad \text{s}^{-1} \tag{4}$$

The electron and neutral densities appearing in Eq. (2) are calculated by using the saturated vapor properties from the Clausius-Clapeyron relation and by letting the vapor expand through a Knudsen layer.[10,11] It was found in Ref. 7 that n_e

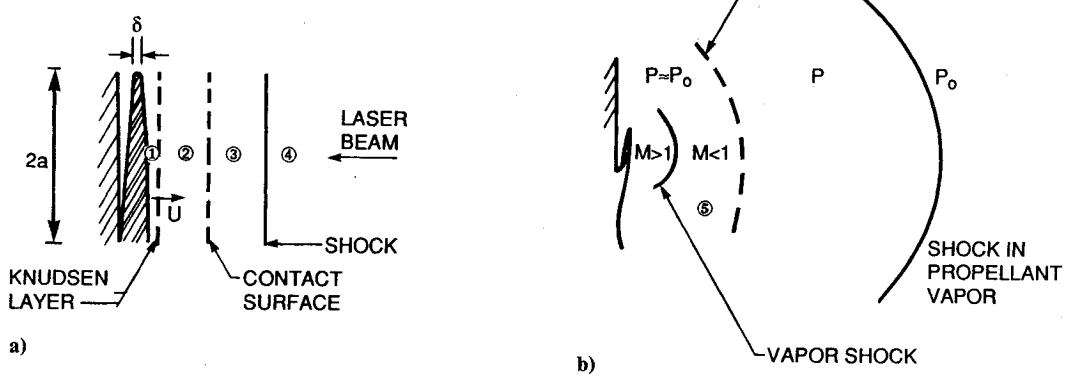

Fig. 4 Geometry fro vapor breakdown: a) one-dimensional expansion, b) three-dimensional expansion (regions 1, 2, and 5 correspond to metal vapor). Breakdown is expected to occur first in region 2 (one dimensional) or 5 (three dimensional).

and n could be expressed as a function of $I_0(\mathrm{W/cm^2})$ as follows:

$$n_e = 6.5 \times 10^{15} \left(\frac{I_0}{10^7}\right)^{1.51} \quad (\mathrm{cm^{-3}}) \tag{5}$$

$$n = 2.6 \times 10^{19} \left(\frac{I_0}{10^7}\right)^{1.01} \quad (\mathrm{cm^{-3}}) \tag{6}$$

Inserting these values of the various physical parameters from Eqs. (3) and (6) into Eq. (2), making the reasonable assumption (see Ref. 7) that $\sigma_1/\sigma_I \simeq 1$, and making $\lambda = 10.6\ \mu$, one obtains

$$\tau_{vbr} = \frac{4.8 \times 10^{-7}}{(I_0/10^7)^{2.25}} \quad (\mathrm{s}) \tag{7}$$

The threshold for breakdown in the one-dimensional regime is now obtained by setting $\tau_{vbr} = \tau_{\exp}(= 3 \times 10^{-9}$ s for a 5-μ radius flake). One finds

$$I\mathrm{th} = 10^8 \times \left(\frac{5}{a}\right)^{0.44} \quad (\mathrm{W/cm^2}) \tag{8}$$

where a is in microns.

Since the breakdown time is so short, the fluence required to break down will be small. For a 5-μ flake, the breakdown fluence is calculated to be 0.35 J/cm^2; i.e., only 10% of the fluence per unit area required to heat a flake to the vaporization temperature.

Plasma Coalescence Time

In order to form a detonation wave it is required that all of the plasma ignition sites grow and coalesce to form a uniform plasma front. Plasmas will initially grow by expansion of the ionized gas and by radiative transfer to the surrounding gas. Inverse bremsstrahlung absorption by photoelectrons generated by deposition of *UV* radiation in the ionized gas surrounding the plasmas will sustain the growth. The problem of modeling the early stages of growth after ignition is complex, and at this stage we can only present rough estimates of this growth. Complete ionization of the aluminum vapor will lead to an overdense plasma at $\lambda = 10.6\ \mu$ ($n_{\mathrm{crit}} = 10^{19}$ cm^{-3}) if I exceeds 10^7 W/cm^2. This will occur when the temperature exceeds 12,000 K. If we assume that the plasma expands at sonic velocity, we obtain an expansion velocity of 3×10^5 cm/s. However, the expanding plasma drives a shock through the surrounding vaporized propellant, which tends to slow down the expansion. Since IB absorption per unit mass scales linearly with ρ, the more the expansion is impeded by the surrounding gas, the greater the heating rate of the plasma. One expects the expansion in the early stages to be similar to a blast wave with continuous energy input from the laser beam. The blast wave will envolve into a detonation wave when the shock is strong enough *and* the amount of partially ionized material between the shock and the aluminum plasma core is large enough to start attenuating the radiation that reaches the core. Lencioni[23] took fast-framing camera pictures of laser-supported detonation waves ignited off aerosols suspended in air which showed that they expanded radially at half the Raizer velocity:

$$v_r = \frac{1}{2} D = \frac{1}{2}\left[2\frac{(\gamma^2 - 1)I_0}{\rho_0}\right]^{1/3} \tag{9}$$

where γ is defined by

$$H - H_0 = \frac{p}{\rho}\frac{\gamma}{\gamma - 1} \tag{10}$$

The velocity v_r is, in effect, the sonic velocity at the Chapman-Jouget conditions, which are reached asymptotically behind the shock.

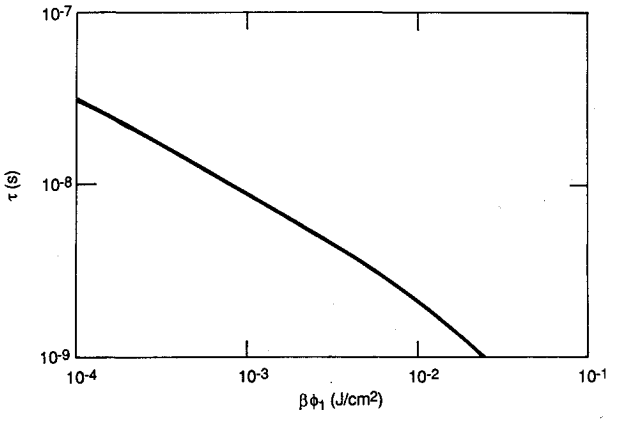

Fig. 5 Plasma coalescence time.

As will be shown in the section on maintenance threshold of LSD waves, an LSD wave has a finite thickness L over which absorption of laser radiation takes place. Therefore, for an LSD wave to be well established there must be a minimum mass per unit area in the wave for almost complete absorption of laser radiation. If M is this minimum mass per unit area, then the time to establish the wave will be of order M/D. As an example, which will be discussed in more detail, consider an LSD wave in water vapor with 1% Li seed, $\rho_0 = 2 \times 10^{-3}$ g/cm^3 and $I_0 = 8.8 \times 10^7$ W/cm^3. Its structure is shown as curve 4 of Fig. 9. We have $L \sim 0.01$ cm, $M = 10^{-4}$ g/cm^2, and $D = 8 \times 10^5$ cm/s. One derives from these numbers a time to form the wave $\tau = M/D = 1.2 \times 10^{-10}$ s and a fluence to establish the wave $I_0\phi = 0.02$ J/cm^2. The radial expansion velocity of the wave is $\sim 4 \times 10^5$ cm/s, which is comparable to the sound velocity of a 12,000 K aluminum plasma that we calculated previously.

We calculate the time for plasma overlap as follows. The area of each plasma centered on a flake, in a plane perpendicular to the laser beam, will grow with time as

$$A(t) = \pi\left[a + \int^t v_r(t')\,\mathrm{d}t'\right]^2$$

The plasma overlap time τ is given by the condition

$$n_f\pi\left[a + \int_0^\tau v_r(t')\,\mathrm{d}t'\right]^2 = 1 \tag{11}$$

where τ is measured from the time to break down.

Let $\beta(\ll 1)$ be the mass fraction of aluminum flakes in the propellant:

$$\beta = \frac{\rho_f}{\rho_p}\pi a^2 N\mathrm{d} \tag{12}$$

If a mass $M(=\phi_1/H_v)$ per unit area of propellant has been vaporized by the first pulse, then the number per unit area of flakes exposed to the second pulse is

$$n_f = \frac{\beta M}{\pi a^2\,\mathrm{d}\rho_f} \quad (\mathrm{cm^{-2}}) \tag{13}$$

Solving Eq. (6) for τ and using the expansion velocity given by Eq. (4), we obtain

$$\tau = \left[\left(\frac{1}{n_f\pi}\right)^{1/2} - a\right]v_r^{-1} = \frac{\left(\dfrac{a^2\mathrm{d}\rho_f H_v}{\beta\phi_1}\right)^{1/2} - a}{\left(\dfrac{(\gamma^2 - 1)I}{4\rho_0}\right)^{1/3}} \tag{14}$$

Consider Eq. (14) under the conditions $I_0 = 10^8$ W/cm^2, $\rho_0 = 1 \times 10^{-3}$ g/cm^3, $a = 5\ \mu$, $H_v = 2$ kJ/g (H_2O), $\rho_f = 2.7$ g/cm^3, and $\gamma = 1.2$. The results are shown in Fig. 5. Figure 5 shows, for example, that for $\phi_1 = 3$ J/cm^2 and $\beta = 10^{-3}$, the plasmas, once ignited, will have coalesced after 5×10^{-9} s. Having chosen $I = 10^8$ W/cm^2, we find that this corresponds to an extra fluence per unit area of 0.5 J/cm^2 that has to be added to the fluence of 3 J/cm^2 required to start vaporizing the flakes and to the fluence 0.1 J/cm^2 required to ignite the plasmas. Thus, the total fluence required to form detonation waves for this case is 3.6 J/cm^2, and the elapsed time is 36 ns.

Maintenance Threshold of LSD Waves

After ignition of a plasma, a LSD wave will propagate in a direction counter to the laser beam and process the propellant vapor that has been generated by the previous pulse. The structure of the LSD wave is shown in Fig. 6. We have a shock propagating through the propellant at velocity D. Behind the shock there is an absorption zone where the laser energy is absorbed. Following strong shock theory the compression ratio across the shock is $\rho_{sh}/\rho_0 = (\gamma' + 1)/(\gamma' - 1)$, where γ' is defined by Eq. (10) for conditions behind the shock. The density decreases as one travels away from the shock until it reaches the asymptotic Chapman-Jouguet condition[3] $\rho_{CJ}/\rho_0 = (\gamma + 1)/\gamma$. For a perfect gas $\gamma = \gamma'$. For an imperfect gas, however, as shown in Ref. 13, the relation $\rho_{CJ}/\rho_0 = (\gamma + 1)/\gamma$ still holds with good accuracy if one defines γ by Eq. (10), using Chapman-Jouguet conditions for H, p, and ρ. In contrast to laser-supported combustion (LSC) waves,[7] where radiation transport plays an important role in the propagation of the wave, LSD waves are hydrodynamic in nature and require that ionization buildup by direct absorption of laser photons. This requires that there be some ionization behind the shock. The degree of ionization behind the shock determining how much electron-neutral inverse bremsstrahlung absorption occurs will determine the thickness of the LSD wave, i.e., the distance between the shock and the absorption zone. Though under typical operating conditions the temperature in the absorption zone is expected to be quite high ($T \geq 12{,}000$ K) and the absorption length to the laser radiation quite small ($1 < 100\ \mu$), the temperature behind the shock is much smaller ($T \leq 6000$ K) and the absorption length much longer ($1 > 1$ mm). A means to decrease this absorption length and, concurrently, to reduce the threshold irradiance for maintaining an LSD wave is to add a small amount of easily ionizable seed such as Na, Li, etc., in the propellant. The seed would be significantly ionized behind the shock and allow more absorption to occur bringing the temperature up to values at which ionization of the propellant species takes over. We can treat the seed as a perturbation on the thermodynamics and fluid dynamics. Assume that a steady LSD wave is propagating through the (vaporized) propellant at velocity D. Conservation of mass and momentum in the frame of the wave takes the form

$$\rho U = \rho_0 D \tag{15}$$

$$p + \rho U^2 = p_0 + \rho_0 D^2 \tag{16}$$

Solution of Eqs. (10) and (11) leads to the Maxwell line in p/p_0 vs $\eta = (\rho_0/\rho)$ space shown in Fig. 6. All of the points in the LSD wave lie on the segment of the line that extends from η_{sh} to η_{CJ}. In order to find the Chapman-Jouguet conditions we must add the conservation of energy equation:

$$H + \frac{1}{2}U^2 = H_0 + \frac{1}{2}D^2 + \frac{I_0}{\rho_0 D}\left(1 - \exp - \int^x k\ dx'\right) \tag{17}$$

The last term in Eq. (17) represents the energy per unit mass absorbed by the propellant at a distance x in the wave measured from the shock front. The Chapman-Jouguet conditions are only reached asymptotically. They correspond to that point on the Maxwell line where $x \to \infty$ and $\exp - \int^x k\ dx' \to 0$, so that the last term in Eq. (17) is $I_0/(\rho_0 D)$. The solution to Eqs. (15–17) is carried out as follows. We rewrite Eq. (17) as

$$H + \frac{1}{2}U^2 - H_0 - \frac{1}{2}D^2 = \frac{I_{abs}}{\rho_0 D} \tag{18}$$

Since H is a function of p and ρ, the right-hand side of Eq. (18) is perfectly specified as we go down the Maxwell line from point A. Elimination of U and D from Eqs. (15), (16), and (18) yields a family of Hugoniot curves for various values of I. These curves are shown schematically in Fig. 7. It is well known that the Chapman-Jouguet point corresponds to the point at which the Hugoniot curve is tangent to the Maxwell line.[13] Although the normal procedure for studying LSD waves[13] is to fix I_0, calculate the Hugoniot curve corresponding to this I_0, and find the point of tangency of this curve with a line originating from point B ($\eta = 1$, $p/p_0 = 1$), we use the opposite procedure. We fix D, i.e., the slope of the Maxwell line, and evaluate the right-hand side of Eq. (18) as we march down the Maxwell line from point A. The value of I_{abs}, which corresponds to the irradiance absorbed, increases until it reaches a maximum $I_{abs} = I_0$ corresponding to Chapman-Jouguet conditions, and then decreases as one goes to larger (unphysical) values of ρ_0/ρ. The laser irradiance in our approach is a derived quantity. However, in order to obtain an approximate value for I_0, one can use the results of a constant γ approximation to the gas properties, where γ is defined by Eq. (10). One would then solve Eq. (9) for I_0 as a function of D.

In order to determine the structure of the LSD wave, we need a length scale along the Maxwell line. This is determined by the magnitude of the absorption coefficient. From the equation of state of the propellant, assuming equilibrium conditions, one can determine T and also the degree of ionization as a function of p and ρ, i.e., as a function of location on the Maxwell line (ML). The absorption coefficient k which is due to electron-neutral and electron-ion collisions, can therefore readily be determined. Since

$$\left(\frac{dI}{d\eta}\right)_{ML} = \frac{d}{d\eta}\left[I_0(1 - \exp - \int^x k\ dx')\right]_{ML} = k(I_0 - I)\left[\frac{dx}{d\eta}\right]_{ML} \tag{19}$$

we can obtain the length scale by integration:

$$x(\eta) = \int_{\eta_{sh}}^{\eta} \frac{(dI/d\eta)\ d\eta}{k(I_0 - I)} \tag{20}$$

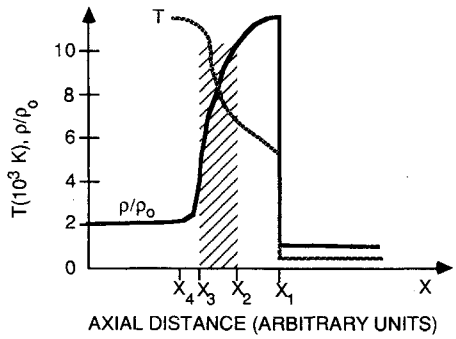

Fig. 6 Structure of laser-supported detonation wave. Laser beam is incident from the right. The wave is traveling toward the right (increasing x). The shock is at x_1; main absorption occurs in the hashed zone between x_2 and x_3. Conditions are close to Chapman-Jouguet for $x < x_4$.

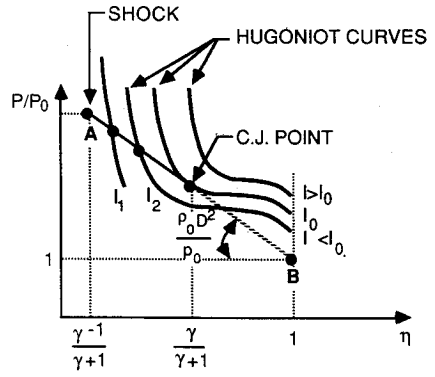

Fig. 7 Integration line for calculating structure of LSD wave.

Though, in principle, the thickness of the LSD waves is obtained by carrying out the integral up to $\eta = \eta_{CJ}$, we cannot carry out the integral because it diverges logarithmically as I approaches I_0. For practical considerations we may define the thickness as that corresponding to a large fraction (e.g., 99%) of the laser beam absorbed and define the upper limit $\eta_{\max}$ as that corresponding to $I_{\max}/I_0 (=0.99)$.

Application to LSD Waves in Various Propellants

Seeded Water

Calculations were performed for LSD waves in water vapor seeded with lithium. Water is a good candidate fuel since it can be stored as ice and leads to a gas with low average atomic weight ($A = 6$ g/mole) after processing through an LSD wave (no molecular recombination is expected upon expansion for the densities and time scales of interest). Also, a low average atomic weight is necessary for high specific impulse. A computer program was written to determine conditions on the Maxwell line. Thermochemical properties of water and its components were obtained from the JANAF tables.[14] These tables, which are valid for $T < 6000$ K, were extended to temperatures up to 20,000 by evaluating partition functions and using the methods described in the introductory chapter to these tables.[14] The code uses, as a subroutine, an equilibrium code that calculates p and h as a function of ρ and T. The constraint $dp/d(1/\rho) = \text{constant}$, which must be satisfied along the Maxwell line, was used to relate ΔT to $\Delta\rho$ as one marches along the line. The k that is needed to determine the length scales can be written as

$$k = \left(\chi_{ej} n_e \sum_j n_j + \chi_{ei} n_e n_i\right)(1 - \exp - h\nu_L/kT) = k_{en} + k_{ei} \tag{21}$$

where the sum over j extends over neutral species. The last bracket in Eq. (16) takes into account stimulated emission. The variable χ_{ei} is given by Kramer's formula[10] (λ in cm)

$$\chi_{ei} = \frac{1.36 \times 10^{-23}}{\sqrt{T}} \bar{Z}^2 \lambda^3 G_F e^{(h\nu_L/kT)} \tag{22}$$

where T is Kelvins, and following Zel'dovich and Raizer,[16] the free-free IB absorption coefficient was augmented by the factor $e^{h\nu_L/kT}$ to include bound-free absorption. The G_F has been calculated by Karzas and Latter[17] and may be taken equal to 1.16 for the wavelength and temperatures of interest.[18] The cross section for electron-neutral IB collisions with oxygen atoms has been calculated quantum mechanically by Geltman[19] and for collisions with hydrogen by Stallcop.[20] We show their results in Fig. 8. For the results presented later the segment AB on the Maxwell line was split into 40 equal intervals in which pure propellant properties and values of I were evaluated. This generated a data file that was used to study the variation of LSD wave structure with amount of seed by use of Eq. (20) after evaluation of k. The electron concentration in the presence of seed was calculated by solving the Saha equation[21]:

$$\frac{n_e[M^+]}{[M]} = 4.8 \times 10^{15} \frac{g^+}{g} T^{3/2} \exp\left(-\frac{\epsilon_I}{k_B T}\right) \equiv B(T) \tag{23}$$

where for lithium ($[M] = [\text{Li}]$)$g^+ = 1$, $g = 2$, and $\epsilon_I = 5.4$ eV. Let c be the molar concentration of seed in the water and y its degree of ionization. We can write to a first approximation that the electron density is the sum of the density due to ionization of pure propellant in the absence of seed and the ionization of seed atoms, i.e.,

$$n_e = n_{e0} + \delta = n_{e0} + cyn \tag{24}$$

Inserting this expression for n_e in Eq. (19) we get

$$\frac{ycn(n_{e0} + ycn)}{(1 - y)cn} = B(T) \tag{25}$$

where $n = \rho(n_{\text{AV}}/18)$ and $n_{\text{AV}} (=6.02 \times 10^{23})$ is Avogadro's number. Equation (25) leads to a second-degree equation for y that can readily be solved. Inserting this value into Eq. (24), we then calculate the increase in electron density due to the presence of seed. The absorption coefficient in the *presence* of seed is

$$k(c) = k_{en}(c = 0)\left(1 + \frac{\delta}{n_{e0}}\right) + k_{ei}(c = 0)\left(1 + \frac{\delta}{n_{e0}}\right)^2 \tag{26}$$

where k_{en} and k_{ei} are the electron-neutral and electron-ion IB absorption coefficients of the propellant (water) in the *absence* of seed and are given by Eq. (21). The approximation that we used in Eq. (24) is expected to be quite good when $\delta \gg n_{e0}$ and $\delta \ll n_{e0}$, but will lead to an error by at most a factor of two in electron density when $\delta \cong n_{e0}$.

We have used Eq. (26) in Eq. (14) to scale LSD waves in pure propellant to waves in which a varying amount of seed has been added. Results are shown in Figs. 9–12. These correspond to initial conditions $\rho_0 = 2 \times 10^{-3}$ g/cm^3 and $D = 8 \times 10^5$ cm/s with lithium seed atom fractions ranging from 0 to 3%. The laser irradiance for $D = 8 \times 10^5$ cm/s was calculated to be $I_0 = 8.8 \times 10^7$ W/cm^2. The calculations were stopped at a distance where 99% of the laser beam has been absorbed.

Figure 9 shows density vs distance. We see from this figure that addition of 0.03% molar concentration of seed reduces the thickness of the LSD wave from 0.24 to 0.06 cm, i.e., by a factor of four. The compression ratio starts out at the shock wave with a value of 9.75 corresponding to a $\gamma = 1.23$ and ends with a value of 1.97 corresponding to a γ of 1.03. Figure

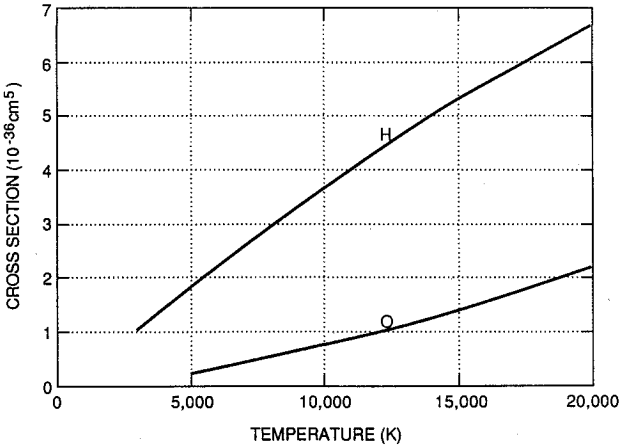

Fig. 8 Electron neutral inverse bremsstrahlung absorption cross section at 10.6 μ for electron collisions with H and O.

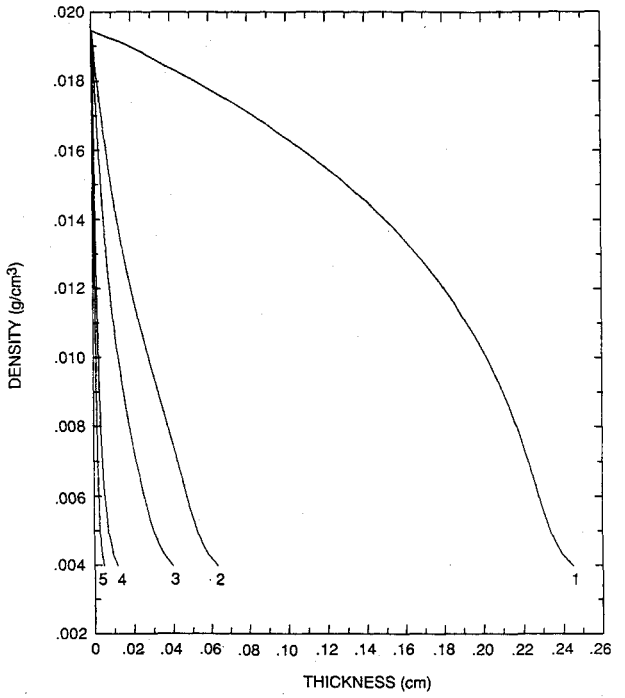

Fig. 9 Density in laser-supported detonation wave in water at $I = 8.8 \times 10^7$ W/cm² and $\rho_0 = 2 \times 10^{-3}$ g/cm³. Curves 1–5 correspond to 0, 0.03, 0.1, 1, and 3% molecular fractions of lithium seed.

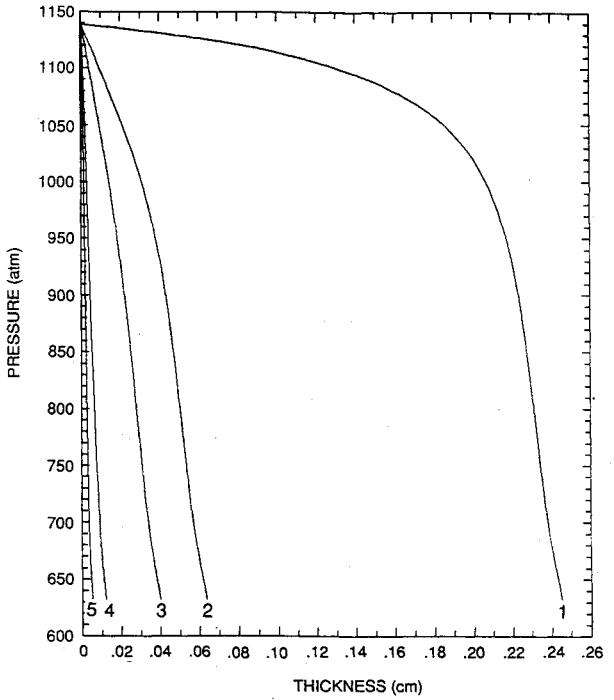

Fig. 10 Pressure in LSD wave. Same conditions as in Fig. 9.

10 shows the pressure in the LSD wave; it decreases by a factor of slightly less than two from shock to Chapman-Jouguet conditions. The temperature, shown in Fig. 11, increases from the shock value of 6700 to a value near 12,000 K. The absorption coefficient in the wave is shown in Fig. 12. It is seen to first increase with distance and then decrease. The decrease in k is due to the rapid decrease in density as one approaches Chapman-Jouguet conditions. Even though the degree of ionization n_e/n increases, this is more than counterbalanced by a decrease in n. This is certainly true at 0.3% seed, where the seed is completely ionized as one approaches the Chapman-Jouguet point, and the decrease in k is due solely to the decrease in n. One sees from

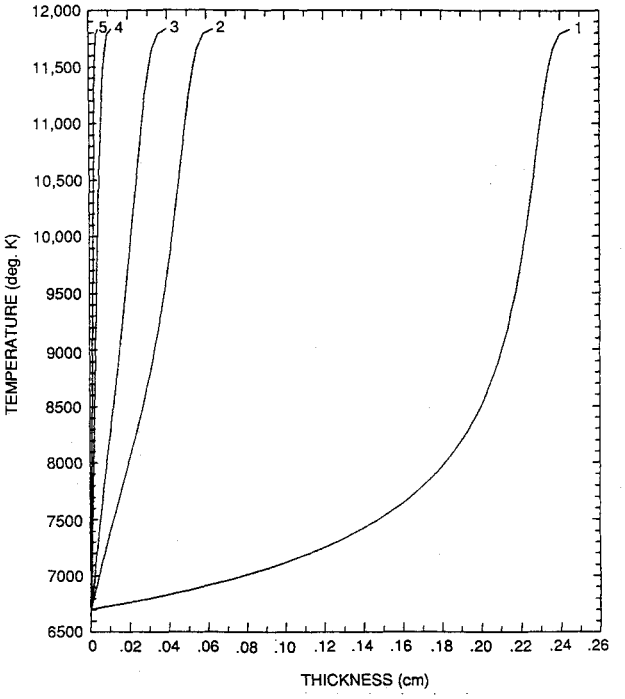

Fig. 11 Temperature in LSD. See Fig. 9 for conditions.

Fig. 12 that the maxima in k for curves 4 and 5 exceed the maximum k for pure propellant (H_2O) up to the Chapman-Jouguet conditions when the concentration of seed exceeds 0.3–1%.

Lithium Hydride (LiH)

LiH is an interesting propellant because it leads to vapor products with low average molecular weight and because Li, which has an ionization energy of 5.39 eV, is readily ionized at temperatures in excess of 5000 K. When heated, solid LiH decomposes into vapor products following the reaction

$$\mathrm{LiH(s)} \rightarrow \mathrm{Li} + \tfrac{1}{2}\mathrm{H_2} \tag{27}$$

The saturated vapor pressure, obtained by use of an equilibrium code using the JANAF thermochemical data[14] for the solid and vapor products, is well approximated by

$$P_s \quad (\mathrm{atm}) = 1.01 \times 10^5 \exp -(16{,}120/T_S) \tag{28}$$

One readily verifies from Eq. (28) that P_s increases from 0.15 to 8.7 atm as the temperature of the surface increases from 1200 to 1700 K. It is easy with such a propellant to operate in a regime where the plasma formed from ionization of Li is overdense to the CO_2 laser radiation. When this occurs, there will be some reflection of the radiation at the overdense surface, thereby reducing the efficiency of the coupling. If we assume that only lithium becomes ionized, then we can prevent the overdense condition by operating in a regime so that $[\mathrm{Li}] + [\mathrm{Li}^+] < n_c$, where $n_c (= 10^{19}\ \mathrm{cm}^{-3})$ is the critical electron density at the laser wavelength (10.6 μ). This leads to the following condition on the density:

$$\rho_{0c} = \frac{\gamma}{\gamma+1}\rho_{CJ} \leq \frac{\gamma}{\gamma+1}\frac{7.94 n_c}{N_{\mathrm{AV}}} \leq 6.9 \times 10^{-5} \quad \mathrm{g/cm^3} \tag{29}$$

where in the last step we set $\gamma = 1.1$, $n_c = 10^{19}\ \mathrm{cm}^{-3}$, and where we used the fact that there is 1 mole of Li in every 7.94 g of propellant.

Such a low density can be achieved either by operating at low enough irradiance in the first pulse (stage 1 in Fig. 1) so that the density of the vapor leaving the surface satisfies inequality [Eq. (29)] or by allowing a sufficient time between the first and second pulse for the vapor to expand to

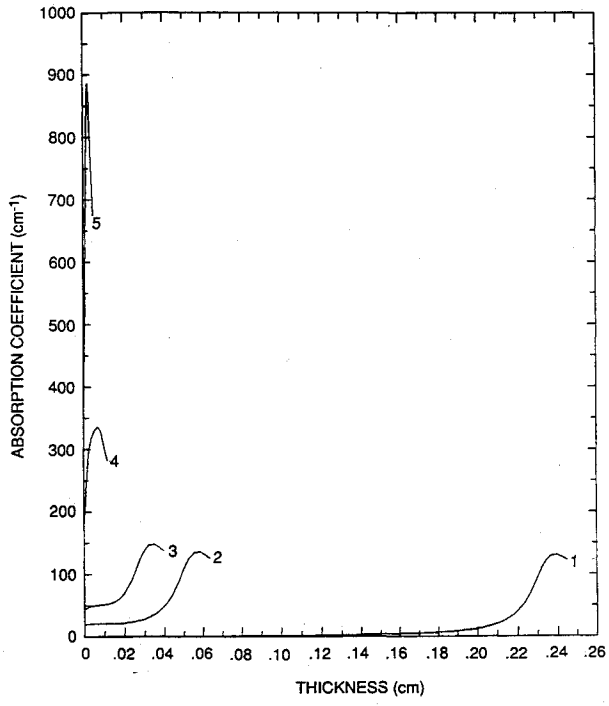

Fig. 12 Absorption in LSD wave. See Fig. 9 for conditions.

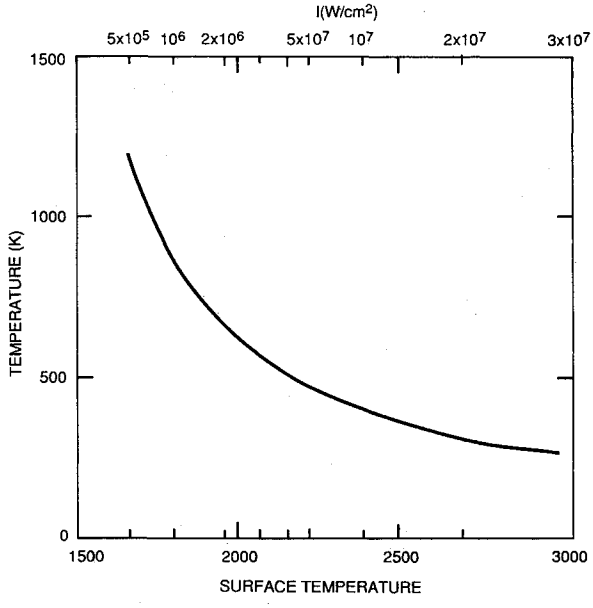

Fig. 13 Temperature in expanded LiH vapor at $\rho = 6.9 \times 10^{-5}$ g/cm³.

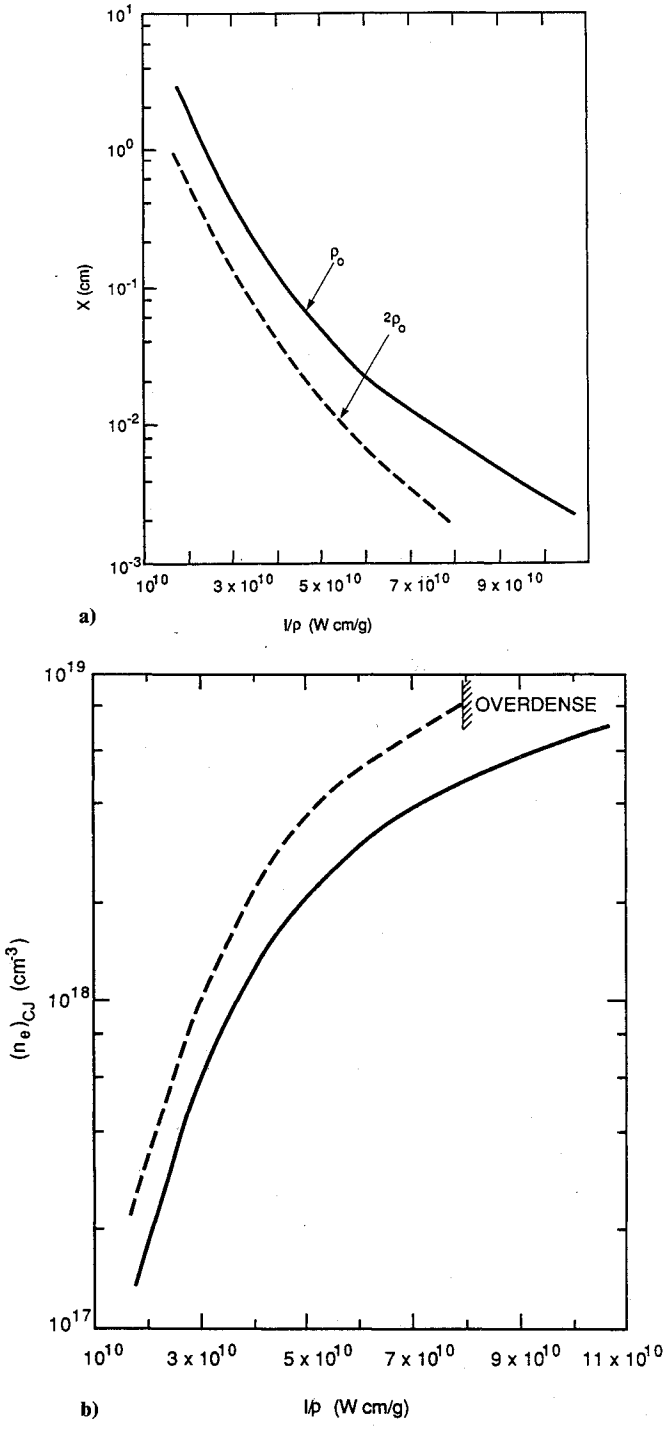

Fig. 14 Properties of LSD waves in LiH vapor for $\rho_0 = 6.9 \times 10^{-5}$ g/cm³. a) Ninety-nine percent absorption thickness. b) Electron density at *CJ* point.

$\rho < 6.9 \times 10^{-5}$ g/cm³. The vapor, upon leaving the surface, expands through the Knudsen layer, which is approximately three mean free paths thick. The half Maxwellian velocity distribution of particles leaving the surface is converted at the edge of the Knudsen layer into a full Maxwellian distribution of particles flowing at a sonic velocity with respect to the surface. Following Anisimov,[10] the temperature and density drop across the Knudsen layer for a monatomic gas ($\gamma = 1.667$) is given by

$$T^* = 0.669\, T_s \tag{30a}$$

$$\rho^* = 0.308\, \rho_s \tag{30b}$$

In the case of saturated LiH vapor we expect that the effective γ for calculating expansion across the Knudsen layer will be $\gamma = 1.55$ ($= 17/11$) if we assume that vibrational degrees of freedom and chemistry are frozen. This slight change in γ will weakly affect the expansion, the factor 0.308 being replaced by 0.305, and 0.669 replaced by 0.725. The threshold irradiance corresponding to $\rho^* = \rho_{0c}$ can then be calculated from the conservation of energy under steady-state vaporization:

$$\dot{m}[H_v(T_s) - H_p] = I\text{th}(1 - R) \tag{31}$$

where $\dot{m} = \rho^* \sqrt{(\gamma k_B T^*/\mu)}$ and $\mu (= 5.29/N_{AV})$ is the average molecular weight of the vapor. Since $P_s = (\rho_s/\mu) k_B T_s$, we can solve Eqs. (28) and (31) for Ith:

$$I\text{th} = 3.3 \times 10^{10} \left(\frac{\mu}{k_B T_s}\right)^{1/2} \frac{\exp -(16{,}120/T_s)[H(T_s) - H_p]}{(1 - R)} \tag{32}$$

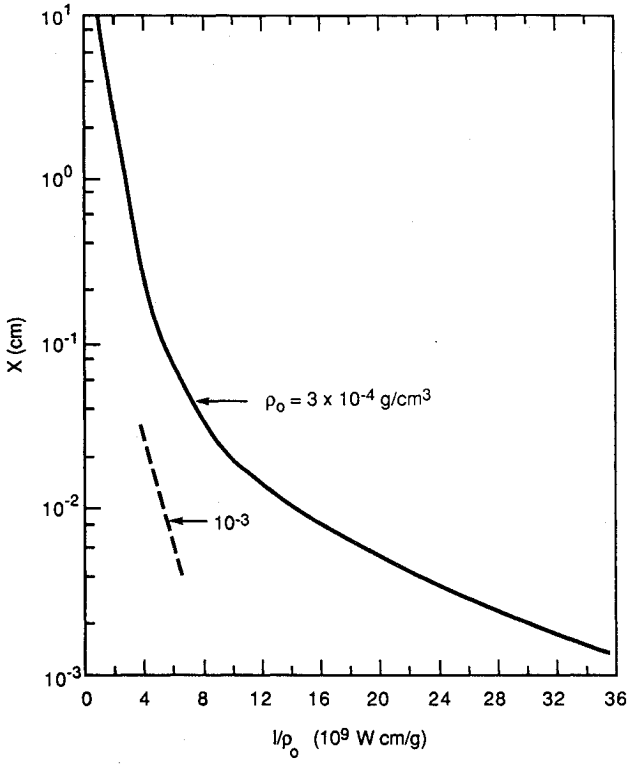

Fig. 15 Ninety-nine percent thickness of LSD wave in glass vapor. $T_0 = 2750$ K; ρ_0 as indicated on curves.

where T_s is given by the solution of

$$\rho^* = 6.9 \times 10^{-5} \quad \text{g/cm}^3 = 0.305\,\rho_s$$

$$= 3.1 \times 10^{10}\left(\frac{\mu}{k_B T_s}\right)\exp(-16.120/T_s) \tag{33}$$

The solution to Eq. (33) is $T_s = 1650$ K. Inserting this value into Eq. (32) and setting $R = 0.05$, $\mu = 8.79 \times 10^{-24}$ g, $H(T_s) - H_p = 3.79 \times 10^4$ J/g. We find that Ith $= 4.7 \times 10^5$ W/cm^2.

If $I > I$th, then the density $\rho^* > 6.9 \times 10^{-5}$ g/cm^3. Before the second pulse is applied the vapor must be allowed to expand adiabatically. We will have

$$T = T^*\left(\frac{\rho}{\rho^*}\right)^{\gamma - 1} = 1.4\,T_s\left(\frac{\rho}{\rho_s}\right)^{0.55}$$

where in the last step we used the results for $\gamma = 1.55$. Setting $\rho = 6.9 \times 10^{-5}$ g/cm^3, we can calculate T as a function of T_s. The result is shown in Fig. 13.

Calculation of LSD waves in LiH was performed using the same algorithm as for seeded water. We show in Fig. 14a the (99% absorption) thickness of the detonation wave as a function of laser irradiance for upstream density $\rho = \rho_0 = 6.9 \times 10^{-4}$ g/cm^3. Figure 14b shows the electron density at the Chapman-Jouguet point. We have also plotted as dashed lines results at double the critical density. The plasma becomes overdense at $I = 1.07 \times 10^8$ W/cm^2 for $\rho = 2\rho_0$.

Glass

We have carried out calculations on glass because LSD waves are readily ignited in vaporized glass products and can be maintained at relatively low laser irradiances. Though the specific impulse is expected to be quite low because of the high average molecular weight of the vapor products, the ease with which experiments can be carried out at low laser pulse energies makes glass an interesting material to compare propellant performance with theoretical calculations. Experiments investigating LSD waves in a soda lime glass have been reported earlier.[22]

We show in Fig. 15 calculations of LSD wave thickness in a soda lime glass of composition $(SiO_2)(Na_2O)_{0.19}(CaO)_{0.14}$. Glass has a short absorption depth of 5 μ at $\bar{\lambda} = 10.6\,\mu$ and is readily vaporized by the first laser pulse when the fluence exceeds 2 J/cm^2. The vapor pressure at 3000 K is 6 atm, and the main vapor component is SiO.

Discussion

Previous assessments of the case for ground to orbit laser propulsion[19] suggest that such a system will be superior to chemical rockets when the specific impulse (impulse per unit weight of propellant consumed) reaches about 800 s and the efficiency (directed kinetic energy of exhaust gases divided by input laser energy) approaches 40%.

The hydrodynamics of detonation wave propagation in realizable exhaust gas distributions require that the laser pulse duration be less than or about 1 μs, whereas considerations of beam propagation through the atmosphere require peak irradiance to be less than about 10^8 W/cm^2 (depending on the wavelength). The combination of these constraints yields the requirement that propellant mass processed per cycle will be less than or about 1 mg/cm^2. The amount of not fully processed mass that remains in the wave at the time that it reaches the edge of the exhaust gas distribution must be small compared to the total processed mass. Allowing a factor of 10 for this consideration yields an estimate that, for a reasonable thruster, the detonation wave should only contain less than or about 100 μg/cm^2. It is clear from Fig. 8 that only the curves corresponding to the relatively high seed percentages of 1 and 3% readily meet this condition. The difficulty is even more pronounced at lower irradiance.

Considerable progress has been made toward understanding the laser-propellant interactions that will occur in laser supported detonation wave thrusters for ground to orbit vehicle launch. Results suggest that suitable propellants can be realized, but must be carefully engineered. In the section on prompt ignition of plasma a specific scheme was presented that can yield plasma ignition at reasonable fluences. However, the scheme requires that a significant number of local ignition sites, such as thin flakes of aluminum, be dispersed throughout the propellant during manufacture. In the section on maintenance threshold of LSD waves we have shown that maintenance of the detonation wave will require that the propellant include a high percentage of a low ionization potential element. This, too, presents a significant challenge to the propellant designer. Other propellant requirements are that it must be structurally strong to withstand the repeated impulsive loads encountered on each thrust cycle, it must be of low average atomic weight to obtain the desired specific impulse, and it must be highly opaque to the laser beam so that the solid does not melt from an excessive heat load accumulated from pulse to pulse in the repetitive train that is likely to last about 10 min. Ongoing experimental work is focused on the design, fabrication, and proof testing of a suitable propellant.

References

[1]Pirri, A. N., and Weiss, R. F., "Laser Propulsion," AIAA Paper 72-719, June 1972.

[2]Douglas-Hamilton, D. H., Kantrowitz, A. R., and Reilly, D. A., "Laser Assisted Propulsion Research," *Progress in Astronautics and Aeronautics: Radiation Energy Conversion in Space*, Vol. 61, AIAA, New York, 1978, pp. 217–278.

[3]Raizer, Y. P., "Heating of a Gas by a Powerful Laser Pulse," *Soviet Physics JETP*, Vol. 21, Nov. 1965, pp. 1009–1017.

[4]Reilly, J., Singh, P., and Weyl, G., "Multiple Pulse Propagation Through Atmospheric Dusts at 10.6 Microns," AIAA Paper 77-697, June 1977.

[5]Zel'dovich, Y. B., and Raizer, Y. P., "Cascade Ionization of a Gas by a Light Pulse," *Soviet Physics JETP*, Vol. 70, 1965, pp. 772–780.

[6]Walters, C. T., Barnes, R. H., and Beverly, R. E., III, "Initiation of Laser Supported Detonation (LSD) Waves," *Journal of Applied Physics*, Vol. 49, May 1978, pp. 2937–2949.

[7]Weyl, G., Pirri, A. N., and Root, R., "Laser Ignition over Aluminum Surfaces," *AIAA Journal*, Vol. 19, April 1981, pp. 460–469.

[8]Zel'dovich, Y., and Raizer, Y., *Physics of Shock Waves and High Temperature Hydrodynamic Phenomena*, Vol. 1, Academic, New York, 1966, p. 283.

[9]Hyman, H., Kivel, B., and Bethe, H., "Inverse Neutral Bremsstrahlung for Highly Polarizable Systems," Avco Everett Research Lab., Everett, MA, Rept. AMP333, 1966.

[10]Anisimov, S., "Vaporization of Metal Absorbing Laser Radiation," *Soviet Physics JETP*, Vol. 27, July 1968, pp. 182–183.

[11]Knight, C., "Theoretical Modeling of Rapid Surface Vaporization with Backpressure," *AIAA Journal*, Vol. 17, May 1974, pp. 519–523.

[12]Raizer, Y. P., "The Feasibility of an Optical Plasmatron and its Power Requirements," *Soviet Physics JETP Letters*, Vol. 11, May 1970, pp. 302–305.

[13]Weyl, G., and Shui, V., "Laser Supported Detonation Waves in Gases," *Proceedings of 11th International Shock Tube Symposium*, University of Washington Press, Seattle, 1978, pp. 577–587.

[14]JANAF Thermochemical Tables, NSRDS-NBS-37, U.S. Government Printing Office, Washington DC, 1971.

[15]Zel'dovich, Y. B., and Raizer, Y. P., *Physics of Shock and High Temperature Hydrodynamic Phenomena*, Academic, New York, 1966, p. 259.

[16]Zel'dovich, Y. B., and Raizer, Y. P., *Physics of Shock and High Temperature Hydrodynamic Phenomena*, Academic, New York, 1966, pp. 271–272.

[17]Karzas, W. J., and Latter, R., "Electron Radiative Transitions is a Coulomb Field," *Astrophysical Journal, Supplemental Series*, Vol. 6, May 1961, pp. 167–212.

[18]Shkarovsky, I., Johnston, T., and Bashynski, M., *The Particle Kinetics of Plasma*, Addison-Wesley, Reading, MA, 1966, p. 229.

[19]Geltman, S., "Free-Free Radiation in Electron-Neutral Atom Collisions," *Journal of Quantitative Spectroscopy & Radiative Transfer*, Vol. 13, July 1973, pp. 601–613.

[20]Stallcop, J., "Absorption of Infrared Radiation by Electrons in the Field of a Neutral Hydrogen Atom," *Astrophysics Journal*, Vol. 187, Jan. 1974, p. 179.

[21]Zel'dovich, Y. B., and Raizer, Y. P., *Physics of Shock and High Temperature Hydrodynamic Phenomena*, Academic, New York, 1966, p. 444.

[22]Rollins, C., Bailey, A., Gelb, A., Resendes, D., and Weyl, G., "Evaluation of Laser Supported Detonation Wave Thrusters," AIAA Paper 89-1914, June 1989.

[23]Lencioni, D., and Petingill, L., "Dynamics of Particle Induced Breakdown in a Laser Beam," *Optics Research*, Massachusetts Inst. of Technology Lincoln Lab, Vol. 2, April 1974, pp. 23–27.